Global Journal of Pure and Applied Mathematics.
ISSN 0973-1768 Volume 14, Number 4 (2018), pp. 517–534

http://www.ripublication.com/gjpam.htm

Similarity Solution of Unsteady Boundary Layer Flow of Nanofluids past a Vertical Plate with Convective Heating

Wafula Maurine Maraka

Department of Mathematics,
Pan African University, Institute of Basic Sciences,
Technology and Innovation, P.O Box 62000-00200, Nairobi, Kenya.

Kinyanjui Mathew Ngugi and Kiogora Phineas Roy

Department of Pure and Applied Mathematics,
Jomo Kenyatta University of Agriculture and Technology,
P.O Box 62000-00200, Nairobi, Kenya.

Abstract

In tis paper, the behaviour of unsteady state boundary layer flow of nanofluid flowing past an accelerating vertical plate has been investigated numerically. The fluid is a water based nanofluid containing three different types of nanoparticles; Titanium dioxide (TiO_2), Copper(Cu) and aluminium (iii)oxide. The governing non-linear partial differential equations (PDEs) are transformed into a system of nonlinear ordinary differential equations (ODEs) using similarity variables. The resulting boundary value problem is solved using a numerical shooting technique with Runge-Kutta-Fehlberg integration scheme. The effect of solid volume fraction,type of nanoparticle,Eckert number Ec, Magnetic parameter M, Biot number and unsteadiness parameter on the nanofluid velocity, skin friction, temperature and heat transfer characteristics are presented graphically and in tables then quantitatively discussed. The results show that there are significant effects of pertinent parameters on the flow fields.

Nomenclature

(u, v) – Velocity components
(x, y) – Coordinates
T_∞ – Free stream temperature
T_w – Plate surface temperature
T – Temperature

U_w – Plate uniform velocity
U_∞ – Free stream velocity
C_p – Specific heat at constant pressure
k_s – Solid fraction thermal conductivity
k_{nf} – Nanofluid thermal conductivity

Greek symbols

σ – the Stefan-Boltzman constant
η – Similarity variable
Ψ – Stream function
ϕ – Solid volume fraction
μ_f – base fluid dynamic viscosity
μ_{nf} – Nanofluid dynamic viscosity
v_f – base fluid kinematic viscosity
α_{nf} – nanofluid thermal diffusibility
ρ_s – Solid fraction density
ρ_{nf} – Nanofluid density

AMS subject classification:
Keywords: Nanofluids, Boundary layer flow, similarity solution, vertical plate.

1. Introduction

Nanofluids can be described as a colloidal suspension of nanoparticles (1–100 nm) scattered uniformly in a base fluid. The nanoparticles are made from materials that are chemically stable like metals, oxides ceramics, carbides and non metals such as graphite and carbon nanotubes. The commonly used base fluids are ethylene, water, oils and lubricants. Choi [1] who was working with a group of Argonne National Laboratory USA, introduced the term Nanofluid in 1995. Nanofluids enhance the thermophysical properties of the base fluids used. There is no doubt that nanofluids are more stable,have better wetting, spreading and dispersion properties on solid surface as discussed by Nguyen et al. [2]. Nanofluids are produced in industries by several methods. One of the processes is where the nanoparticles are produced using gas condensation after which they are dispersed into the base fluid. Ultrasound is used in the process in order to make sufficient amalgation of the particles and the base fluids, Wang et al. [3] and Eastman et al. [4]. The work published papers by Li et al. [5] and Ghosh et al. [6] among others simplify the physics of nanofluids. Nanofluids have a wide range of practical applications, they can be used as smart materials to work as heat valve to control the flow of heat. Advanced electronic gadgets experience thermal management challenges from reduction of accessible surface area for heat and high level of heat generation. These challenges can be avoided by either increasing the capacity of heat transfer or by finding an optimum geometry of cooling appliances. Due to their high thermal conductivity and increased heat transfer coefficient, nanofluids can be used for liquid coolant of computer

processors. Previously research has been carried out on nanofluids flow. The recent studies include [[7], [8], [9]] among others. Magnificent reviews on convective transport in nanofluids have been done by Kakac and Pramuanjaroenkij [10] and Buongiorno [11].

In presence of magnetic field, nanofluids have several engineering, industrial and biomedical applications such as cooling of nuclear reactors by liquid sodium and induction flow meter, magnetogravimetric separations, smart fluids for vibration damping, aerodynamic sensors magnetic drug targeting, nanocryosurgery and nanodrug delivery.

Flow in vertical plates is a frequently experienced configuration in thermal engineering equipments, for example, cooling devices of electronics, collector of solar energy and micro-electronic equipments. The heat and mass transfer past a vertical plate in the presence of the magnetic field and convective boundary condition were studied by Makinde and Aziz [12]. Mutuku and Makinde [13] presented the MHD nanofluid flow over a permeable vertical plate with convective heating. Makinde [14] presented a similarity solution for MHD mixed convection flow on a vertical plate with the convective boundary condition. They reported that the temperature profile increases with an increase in Biot number. Al-Nimr and Haddad [15] have described the fully developed free convection in an open-ended vertical plates partially filled with porous material. The combined forced and free convective flow in a vertical plates with viscous dissipation and isothermal-isoflux boundary conditions have been studied by Barletta [16]. Barletta et al. [17] have described a buoyant MHD flow in vertical plates. A uniform magnetic field was applied perpendicular to the plates which was subject to adiabatic and isothermal boundary conditions. He recorded that the joules heat and viscous dissipation increases rapidly with inceasing value of magnetic parameter. Sacheti et al. [18] have studied the transient free convective flow of a nanofluid in a vertical plate, he used finite difference scheme to numerically solve the governing equations. Azhar etal [19] presented free convection flow of some fractional nanofluids over a moving vertical plate with uniform heat flux and heat source, he used exact solution and recorded enhancement of heat transfer for fractional nanofluids. Narahari et al. [20] investigated on unsteady magnetohydrodynamic free convection flow past an accelerated vertical plate with constant heat flux and heat generation or absorption,he used laplace transform to solve the governing equations. Unsteady convection flow of some nanofluids past a moving vertical flat plate with heat transfer was presented by Turkylimazoglu [21]. Loganathan [22] carried out a study on transient natural convective flow past a vertical plate in presence of heat generation. Das and Jana [23] investigated natural convective Magneto-nanofluid flow and radiative heat past a moving vertical plate. The governing equations were solved using laplace transform technique. Magnetic field effects on free convection flow of nanofluids past a vertical semi-infinite flat plate using similarity transformation was presented by Hamad et al. [24].

Boundary layer flow is the most important concept that can help in understanding the transport process. The new edition of the near-legendary textbook by Schlichting [25] presents a comprehensive overview of boundary layer theory and its application with particular emphasis on flow past bodies. The idea of separation in mixed convection flow was first studied by Merkin [26], where he investigated the effect of buoyancy opposing and buoyancy assisting for mixed convection boundary layer flow on a semi-infinite

vertical plate. Hunt and wilks [27] further studied a similar problem. They considered a flat plate heated at a constant heat flux rate.Boundary layer flow and heat transfer of Fictionalized multi-walled carbon nanotubes/water nanofluids over a flat plate was investigated by Safaei *et al.* [28], they reported that the boundary layer thickness increases as free stream velocity decreases or particle volume fraction increases. Tamin et al. [29] investigated mixed boundary layer flow of nanofluid near a stagnation-point on a vertical plate for buoyancy opposing and assisting flows. They used similarity solution but for numerical solution they used fourth order Runge-Kutta-Fehlnberg integration scheme along with shooting technique. Grosan and Pop [30] investigated the axisymmetric mixed convection boundary layer flow past a vertical cylinder. They used similarity solution transformation and bvp4c function from Matlab for numerical calculations.

The present paper investigates boundary layer flow of nanofluids past a vertical plate. The study has been motivated by the need to determine the thermal performance of such a system. A combined effect of Viscous dissipation and joule's heating on the boundary layer flow is investigated. A comparative study between the initially published results and the present results reveals excellent agreement between them.

2. Mathematical formulation

We consider an unsteady two-dimensional laminar MHD boundary layer flow of electrically conducting water based nanofluid containing three types of nanoparticles past a vertical plate. A Cartesian co-ordinate system is chosen with x-axis along the direction of the flow and y-axis is measured normal to the surface of the plate as shown in figure. For the time $t \leq 0$, the fluid is steady. The unsteady fluid start at $t > 0$. A transverse magnetic field of strength $B = B_0(1 - ct)^{1/2}$ is applied parallel to the y-axis, where B_0 is a constant magnetic field.

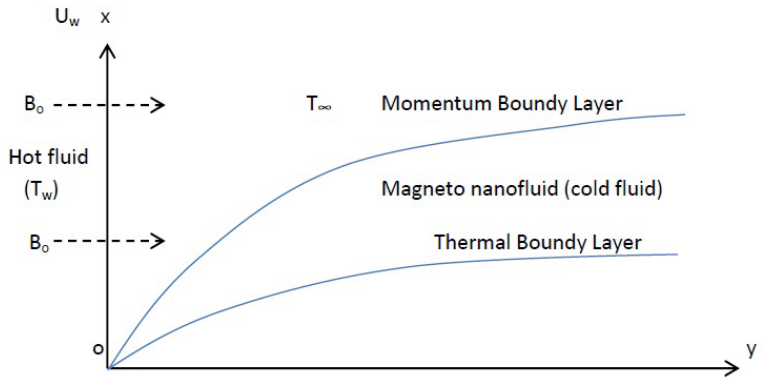

Figure 1: Geometry of the problem

It is assumed that the left side of the plate is heated by convection from a hot fluid at temperature T_w(x) has a linear variation with x and an inverse square law for its decrease with time, while the temperature of the ambient cold fluid is T_∞ with a heat

transfer coefficient h_f. The flow is stable and all body forces except magnetic field are neglected. It is further assumed that the base fluid and the suspended nanoparticles are in thermal equilibrium and no slip occurs between them. The thermo physical properties of water and nanoparticals are given in table 1. All properties are assumed independent of temperature. Further, it is assumed that the suspended nanoparticles and the base fluid are in thermal equilibrium, also it is assumed that the induced magnetic field is negligible in the flow field in comparison with the applied magnetic field, there is also no external electric field applied, so the effect of polarization of the fluid is negligible. Under the above assumptions, the continuity, momentum and energy equations describing the flow are written as [31]

$$\frac{\partial u}{\partial x} = 0 \tag{1}$$

$$\frac{\partial u}{\partial t} + u\frac{\partial u}{\partial x} + v\frac{\partial u}{\partial y} = -\frac{1}{\rho_{nf}}\frac{\partial p}{\partial x} + \frac{\mu_{nf}}{\rho_{nf}}\left(\frac{\partial^2 u}{\partial y^2}\right) - \frac{\sigma_{nf}B_0^2 u}{\rho_{nf}} \tag{2}$$

$$\frac{\partial T}{\partial t} + u\frac{\partial T}{\partial x} + v\frac{\partial T}{\partial y} = \frac{k_{nf}}{(\rho C_p)_{nf}}\frac{\partial^2 T}{\partial y^2} + \frac{\mu_{nf}}{(\rho C_p)_{nf}}\left(\frac{\partial u}{\partial y}\right)^2 + \frac{\sigma_{nf}B_0^2 u^2}{(\rho C_p)_{nf}} \tag{3}$$

Where u and v are the velocity components along the x and y-directions respectively, T is the temperature of the nanofluid, μ_{nf} the dynamic viscosity of the nanofluid, ρ_{nf} the density of nanofluid, σ_{nf} the electrical conductivity of nanofluid, k_{nf} is the thermal conductivity of nanofluid and $(\rho C_p)_{nf}$ is the heat capacitance of nanofluid. The last two terms in equation 3 indicate the effect of viscous dissipation an joule heating respectively. The pressure p is a function of x only.

The, μ_{nf}, ρ_{nf}, $(\rho C_p)_{nf}$ and σ_{nf} as defined by [[32], [33]] are given as;

$$\begin{aligned} \mu_{nf} &= \frac{\mu_f}{(1-\phi)^{2.5}}, \quad \rho_{nf} = (1-\phi)\rho_f + \phi\rho_s \\ (\rho C_p)_{nf} &= (1-\phi)_(\rho C_p)_f + \phi(\rho C_p)_s \\ \sigma_{nf} &= \sigma_f\left[1 + \frac{3(\sigma-1)\phi}{(\sigma+2)-(\sigma-1)\phi}\right] \quad \sigma = \frac{\sigma_s}{\sigma_f} \end{aligned} \tag{4}$$

where; ρ_f is the density of the base fluid, ρ_s is the density of the nanoparticle, ϕ is the volume fraction of the nanoparticle ($\phi = 0$ correspond to a regular fluid or pure water), β_f is the base fluid thermal expansion coefficient, β_s is the nanoparticle thermal expansion coefficient, μ_f is dynamic viscosity of the base fluid, σ_f is electric conductivity of base fluid, σ_s is electric conductivity of nanoparticle, $(\rho C_p)_s$ is the heat capacitance of the nanoparticle and $(\rho C_p)_f$ is the heat capacitance of the base fluid. The expressions in equations 4 are restricted to spherical nanoparticles, where it does not account for other shapes of nanoparticles. These equations were also used by Khanafer et al. [34], Oztop and Abu-Nada [35], and Abu-Nada and Oztop [35]. The Thermophysical properties of the nanofluid are given in Table 1. The effective thermal conductivity of the nanofluid given by Kakac and Pramuanjaroenkij [36] followed by Oztop and Abu-Nada [35] is

given by

$$\frac{k_n f}{k_f} = \frac{(k_s + 2k_f) - 2\phi(k_f - k_s)}{(k_s + 2k_f) + \phi(k_f - k_s)}, \qquad \alpha_{nf} = \frac{k_{nf}}{(\rho c_p)_{nf}} \tag{5}$$

Table 1: Thermophysical Properties of water and nanoparticles [[37], [35]]

Physical properties	Water/base fluid	Cu (Copper)	Al2O3 (Alumina)	TiO2 (Titanium Oxide)
$\rho(kgm^{-3})$	997.1	8933	3970	4250
$C_p(J/KgK)$	4179	385	765	686.2
k(WmK)	0.613	401	40	8.9538
ϕ	0.0	0.05	0.15	0.2
$\sigma(S/m)$	5.5×10^{-6}	59.6×10^{6}	35×10^{6}	2.6×10^{6}

The initial and boundary conditions are [[38]]

$$\begin{aligned} t \leq 0 : u = 0 = v, T = T_\infty \quad for \quad all \quad x, y \\ t > 0 : U_w(x,t) = \frac{ax}{(1-ct)}, v = 0, -k_f \frac{\partial T}{\partial y} = h_f \left[T_w(x,t) - T\right] \ \ at \ \ y = 0, \\ u \to 0, T \to T_\infty \quad as \quad y \to \infty \end{aligned} \tag{6}$$

Where $T_w(x,t) = T_\infty + \dfrac{ax}{(1-ct)^2}$ is the temperature of the hot fluid and a and c are constants (where $a > 0$and $c \leq 0$ with $ct < 1$). These two constants have $time^{-1}$ dimension. The continuity equation (1) is automatically satisfied by introducing a stream function $\upsilon(x, y)$ as,

$$u = \frac{\partial \psi}{\partial y} \ \ , \text{and} \ \ v = -\frac{\partial \psi}{\partial x} \tag{7}$$

The following similarity variables are introduced

$$\eta = y\left[\frac{a}{\upsilon_f(1-ct)}\right]^{1/2}, \quad \psi = \left[\frac{a\upsilon_f}{(1-ct)}\right]^{1/2} x f(\eta), \quad \theta(\eta) = \frac{T - T_\infty}{T_w - T_\infty} \tag{8}$$

Where η is the independent similarity variable, $f(\eta)$ the dimensionless stream function and $\theta(\eta)$ the dimensionless temperature. using equation (7) and (8), we have

$$u = \frac{ax}{1-ct} f'(\eta), \qquad v = -\left[\frac{a\upsilon_f}{(1-ct)}\right]^{1/2} f(\eta) \tag{9}$$

on the use of equation (9) in equations (2) and (3), we obtain the following ordinary differential equations

$$f''' - \phi_1 \left[(f'^2 - ff") + \lambda(f' + \frac{1}{2}\eta f")\right] - \phi_2 Haf' = 0 \tag{10}$$

$$\frac{1}{Pr}\left(\frac{k_{nf}}{k_f}\right)\theta'' + \phi_3\frac{f\theta'}{2} + \frac{Ec}{(1-\phi)^{2.5}}(f'')^2 + HaEc\phi_4 = \lambda(f'-1)^2 = 0 \qquad (11)$$

Where

$$\begin{aligned}
\phi_1 &= (1-\phi)^{2.5}\left[(1-\phi) + \left(\frac{\rho_s}{\rho_f}\right)\right] \\
\phi_2 &= (1-\phi)^{2.5}\left[1 + \frac{3(\phi-1)\phi}{(\phi+2)-(\phi-1)\phi}\right] \\
\phi_3 &= \left[1-\phi+\phi(\rho C_p)_s/(\rho C_p)_f\right] \\
\phi_4 &= (1-\phi+\phi\sigma_s/\sigma_f)(f'-1)^2 = 0
\end{aligned} \qquad (12)$$

and $Ha = \dfrac{\sigma_f B_0^2 x(1-ct)}{\alpha\rho_f}$ is the magnetic parameter representing the ratio of electromagnetic (lorentz) force to the viscous force, $\lambda = \dfrac{c}{a}$ is the unsteadness parameter, $Re_x = \dfrac{U_\infty x}{\upsilon_f}$ is the Reynold's number. $Pr = \dfrac{\upsilon_f}{\alpha_f}$ is the prandtl number and $E_c = \dfrac{U_\infty^2}{C_{pf}(T_w - T_\infty)}$ is the Eckert number. The prime denotes the differentiation with respect to η The corresponding boundary conditions are;

$$f(0) = 0,\ \ f'(0) = 1,\ \ \theta'(0) = -Bi[1-\theta(0)],\ \ f' \to 0,\ \ \theta \to 0,\ \ as\ \ \eta \to \infty. \qquad (13)$$

Where $Bi = \dfrac{h_f}{k_f}\left(\dfrac{(1-ct)x\upsilon_f}{a}\right)^{\frac{1}{2}}$ is the biot number.

Now the Biot number and the magnetic parameter are functions of x. To have similarity equations, all parameters must be a constant and not a function of x. we therefore assume

$$h_f = b\,(x(1-ct))^{-\frac{1}{2}},\ \ \sigma_f = d\,(x(1-ct))^{-1} \qquad (14)$$

where b and d are constants.

2.1. Numerical solution

The governing equations(10) and (11) subject to the boundary conditions (13) were solved numerically by fourth order Runge-Kutta-Fehlberge Method with shooting technique Na [39] and Remeli [40]. Shooting method is chosen to solve the boundary value problem, since it has many advantages such as ease of programming in a general form, less storage is required, and its suitability for automatic procedures. The shooting technique is an iterative algorithm which identifies appropriate initial conditions for a related initial value

problem (IVP) that provides the solution to the original boundary value problem (BVP). For a given boundary value problem, the missing initial conditions is first assumed,and the resulting initial value problem can then be solved by one of the standard foward integration techniques. In this case the fourth order Runge-kutta-Fehlberge method is chosen, which provides accurate results. The accuracy of the assumed initial conditions is then checked by the boundary conditions at the second point. If this boundary conditions is not satisfied, another value may be assumed and the process is repeated again. This process is continued until satisfactory accuracy is achieved. There are systematic methods by which new values of missing boundary conditions can be chosen so that the solution will rapidly converge to the final solution.Such methods include; Newton's method,the parallel shooting method and the method of quasi linearization. In this study, Newton's method is used. The shooting method is based on MAPLE "dsolve" command and MAPLE implementation, "shoot". A detailed explanation of the Shooting method on maple implementation can be found in meade [41]. Computations are carried out for solid volume fraction ϕ. in a range of $0 \leq \phi \leq 0.2$, Magnetic field strength of $10^{-10} \leq Ha \leq 10^{-15}$. The value of the Prandtl number of the based fluid (water) is kept constant at 6.2. In order to validate the accuracy of our numerical procedure, a comparison is made for some of the results obtained from this study with the results of Abolbashari et al. [42] in table 2, there is a great agreement between the values in both studies.

Table 2: Comparison results of $-\theta'(0)$for different values of Prandtl number (Pr) when $Ha = \lambda = 0, \phi = 0.0$ and $Bi \to \infty$

Pr	Abolbashari et al	Present study
0.72	0.80863135	0.80866123
1.00	1.00000000	1.00000000
3.00	1.92368259	1.92367432
7.00	3.07225021	3.07334689
10.0	3.72067390	3.72065437

3. Results and discussion

The effect of various thermo physical parameters on the nanofluid velocity, temperature, heat transfer rate as well as shear stress at the plate are presented in graphs and tables. The Prandtl number for the base fluid(water) is kept constant as Pr=6.2. Computations are carried out for solid volume fraction ϕ in the range $0 \leq \phi \leq 0.2$. $\phi = 0$ for regular fluid and $Ha = 0$ corresponds to absence of magnetic field.

3.1. Effect of parameters on the velocity profiles

Figure 2 reveals the variation in the nanofluid velocity for three types of water-based nanofluids Al_2O_3-water, TiO_2-water and Cu-water. It is noted that there is a increase

in the velocity of the fluid from zero at the plate surface to a maximum value as it proceeds towards the free stream. This condition satisfies the boundary condition. It is also observed that the momentum boundary layer thickness for Al_2O_3-water and TiO_2-water nanofluids are almost the same although TiO_2-water nanofluid exhibits the largest boundary layer thickness. Cu-water nanofluids produced the thinnest momentum boundary layer as seen from **figure 2**. **Figure 3** reveals that the fluid velocity decreases for increasing value of Magnetic parameter Ha. Increasing magnetic parameter also decreases the hydrodynamic boundary layer thickness. This can be explained from the physics of the problem, since the application of a transverse magnetic field results in resistive type of force(Lorentz force) which is similar to drag force which tends to resist the fluid flow and thus reducing its velocity. **Figure 4** shows the influence of volume fraction parameter ϕ on the fluid velocity $f'(\eta)$. The fluid velocity intensifies for increasing values of ϕ. This is because the existence of nanoparticles leads to the thinning of the momentum boundary layer. The effect of unsteadiness parameter λ on the fluid velocity $f'(\eta)$ is clarified from **figure 5**. The reduction of momentum boundary layer thickness is also explained by this. The unsteady motion is $\lambda > 0$ and for steady motion $\lambda = 0$. **Figure 6** displays the effect of eckert number Ec on the fluid velocity.

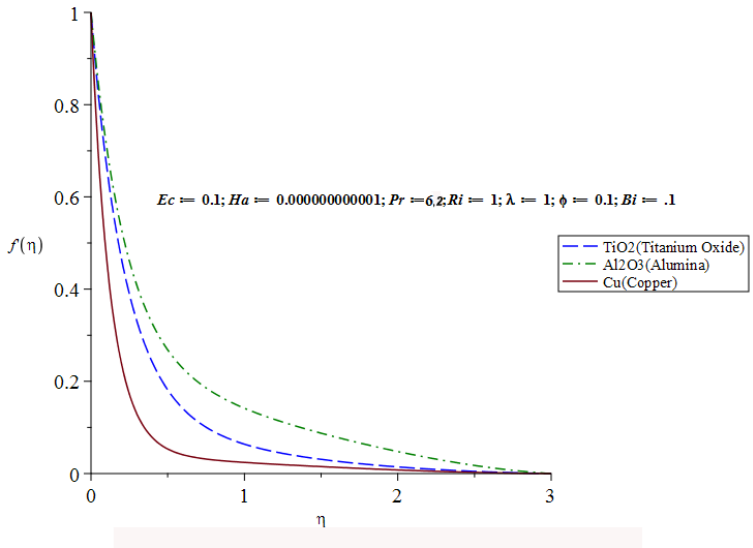

Figure 2: Velocity profile for different nano fluids

3.2. Effects of parameters on tempereture profiles

Figure 7 shows the fluid temperature variations for the three types of water-based nanofluids i.e Al_2O_3-water, Cu-water and TiO_2-water. It is noted that the temperature increases in Cu-water nanofluid. This can be explained from the fact that copper has a high thermal conductivity as compared to Al_2O_3 and TiO_2. It is also noted that the thermal boundary layer thickness is greater for Cu-water nanofluids as compared toAl_2O_3-water and TiO_2-water nanofluids. **Figure 8** presents the effect of volume fraction parameter ϕ on

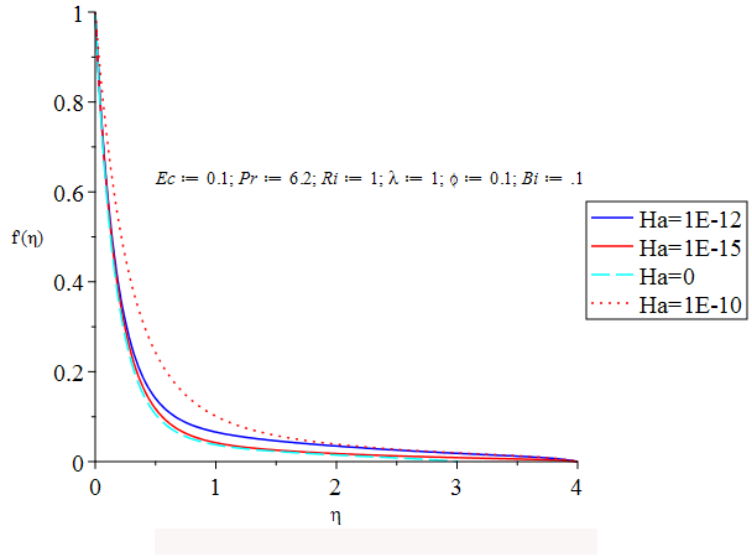

Figure 3: Velocity profile for different magnetic parameter Ha

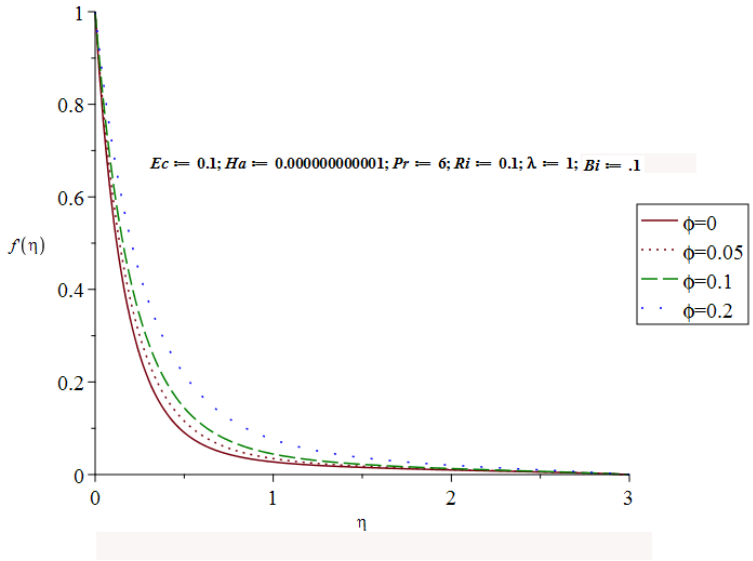

Figure 4: Velocity profile for different nanoparticle volume fraction

the fluid temperature.There is a direct proportion between the temperature and the volume fraction parameter. The fluid temperature $\theta(\eta)$ increases with an increase in volume fraction parameter ϕ. The thermal conductivity of nanofluids is a function of thermal conductivity of both base fluid and nanoparticles. The conductive heat transfer coefficient is enhanced by increasing nanoparticle volume fraction, consequently increase in convective heat transfer. When the volume fraction parameter increases, the thermal conductivity increases and as a result the thermal boundary layer thickness increases.

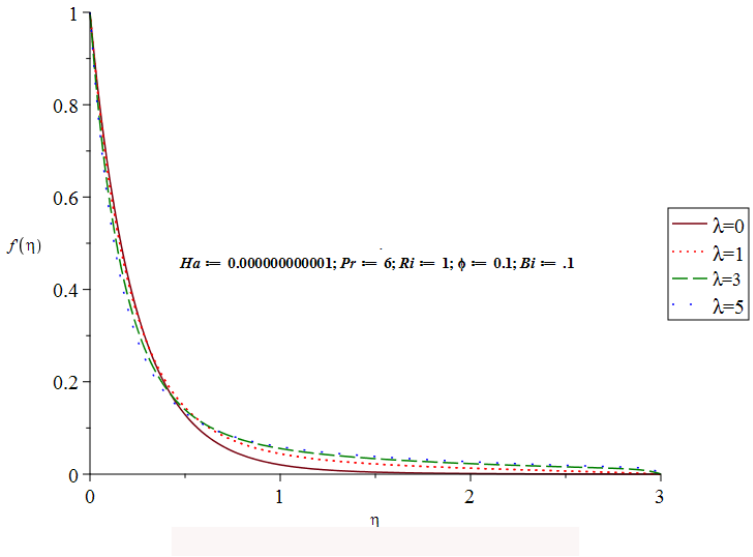

Figure 5: Velocity profile for different λ

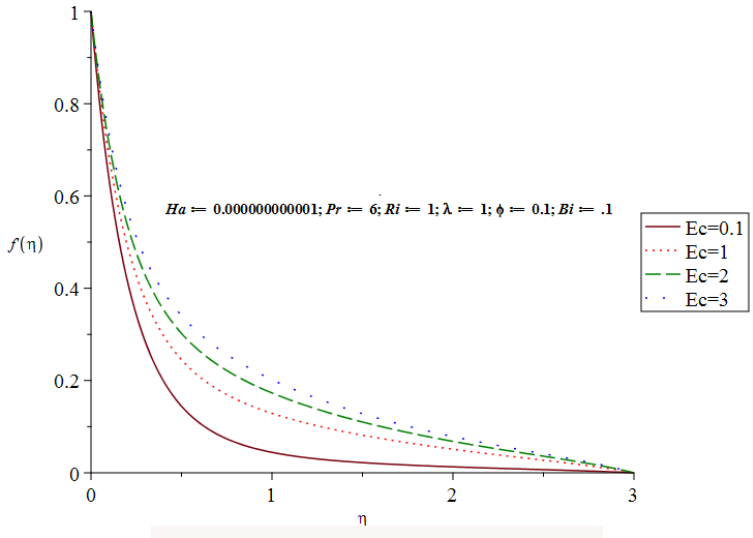

Figure 6: Velocity profile for different Ec

This observation indicates that when nanofluids are used,the temperature changes,this makes the use of nanofluid to be significant in the cooling and heating processes. **Figure 9** demonstrates the effects of unsteadiness parameter λ on the fluid temperature $\theta(\eta)$. As the unsteadiness parameter enlarges,fluid temperature falls near the plate. **Figure 10** displays the effect of Biot number Bi on fluid temperature. It is observed that the fluid temperature rises as the Biot number increases, this leads to an increase in thermal boundary layer thickness. Biot number is the ratio of the hot fluid side convection resistance to the cold fluid side convection resistance on the surface of the plate. In

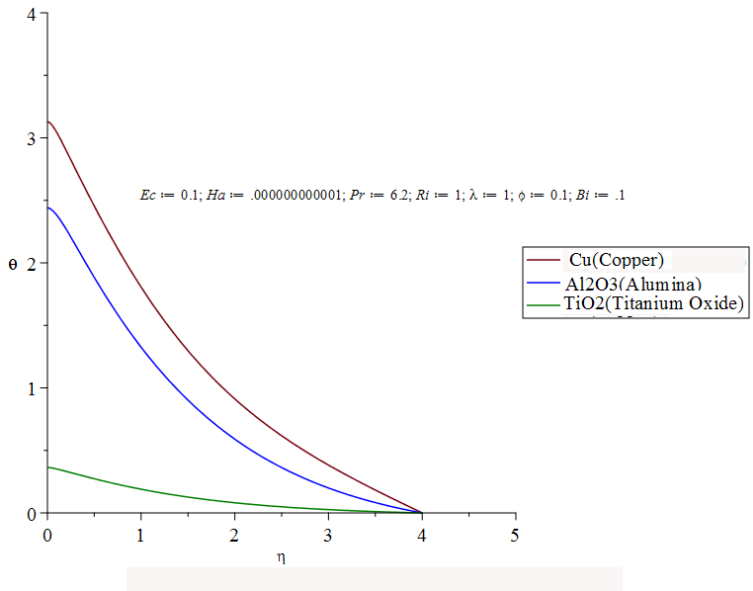

Figure 7: Temperature profiles for different nanofluids

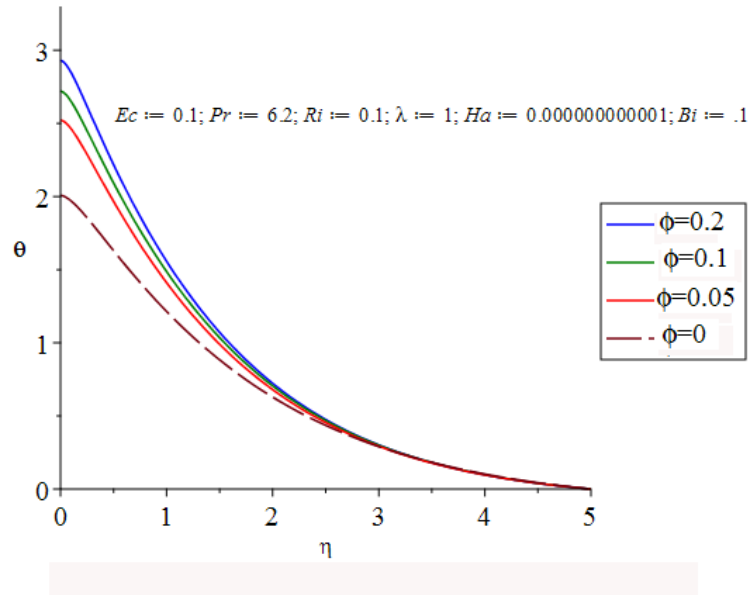

Figure 8: Temperature profiles for different ϕ

case of fixed cold fluid properties, Biot number Bi is directly proportional to the heat transfer coefficient h_f associated with the hot fluid. On the hot fluid side, the thermal resistance is inversely proportional to heat transfer coefficient h_f. The implication for this is that as the Biot Bi number increases, the hot fluid side convection resistance decreases and consequently the surface temperature increases. It is also observed that for

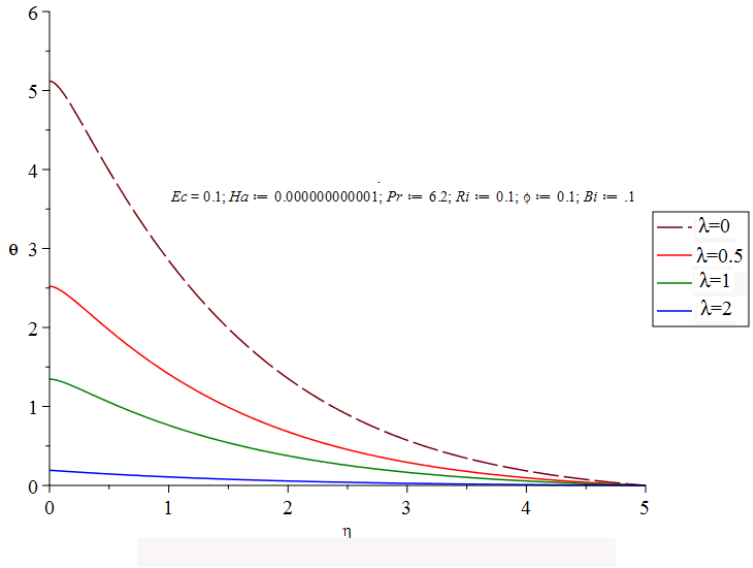

Figure 9: Temperature profiles for different λ

large values of Bi, that is $Bi \rightarrow \infty$, the temperature profile attains its maximum value 1. The convective boundary condition thus becomes the prescribed surface temperature case. When Biot Bi evolves, the thermal boundary layer thickness increases. The larger values of Biot Bi number accompanied with the strong convective heating at the plate rises the temperature gradient at the plate. This allows deeper penetration of the thermal effect in to the quiescent fluid. It is also noted that the fluid temperature 0n the right side of the plate increases with an increase with Biot Bi number, this is because as the Biot number increases, the thermal resistance of the plate decreases and the convective heat transfer to the fluid on the right side of the plate increases. **Figure 11** and **Figure 12** indicates the effect of Eckert (Ec) number and Hartmann number (Ha) on temperature profile respectively. Increase in Eckert number (Ec) and Hartmann number (Ha) leads to an increase in both temperature and thermal boundary layer thickness.

3.3. Effect of parameters on shear stress and rate of heat transfer

The quantities of practical interest in this study are the shear stress and the rate of heat transfer. These parameters characterize the surface drag and heat transfer rate. The numerical values of the shear stress $-f"(0)$ at the plate $\eta = 0$ are recorded in **Table 3** for the three different types of nanoparticles and nanoparticle volume fraction parameter ϕ. It is observed that the shear stress $-f"(0)$ is an increasing function of ϕ for CU-water, Al_2O_3-water and TiO_2-water nanofluids. Consequently, it is noted that the shear stress $-f"(0)$ is higher in the Cu-water nanofluids as compared to the Al_2O_3-water and TiO_2-water nanofluids. This imply that Cu-water nanofluids gives a higher drag force in opposition to the flow as compared to TiO_2-water and Al_2O_3-water nanofluids. The negative value of of f"(0) signifies that the plate surface exerts a drag force on the fluid.

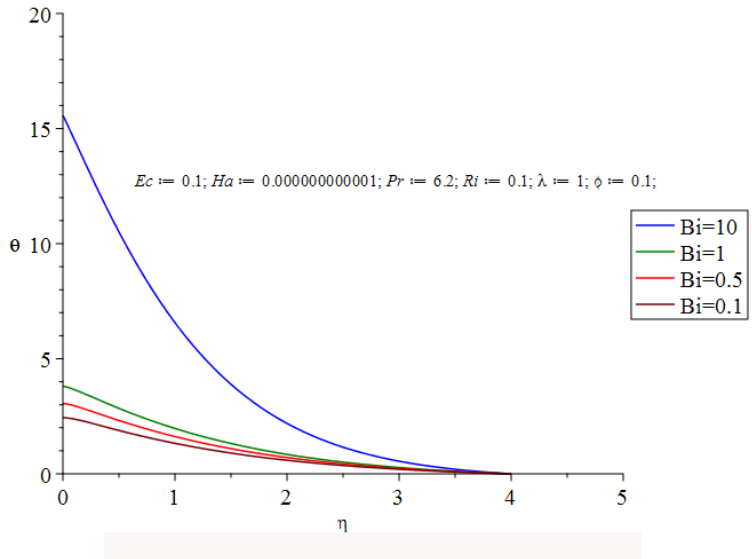

Figure 10: Temperature profiles for different Bi

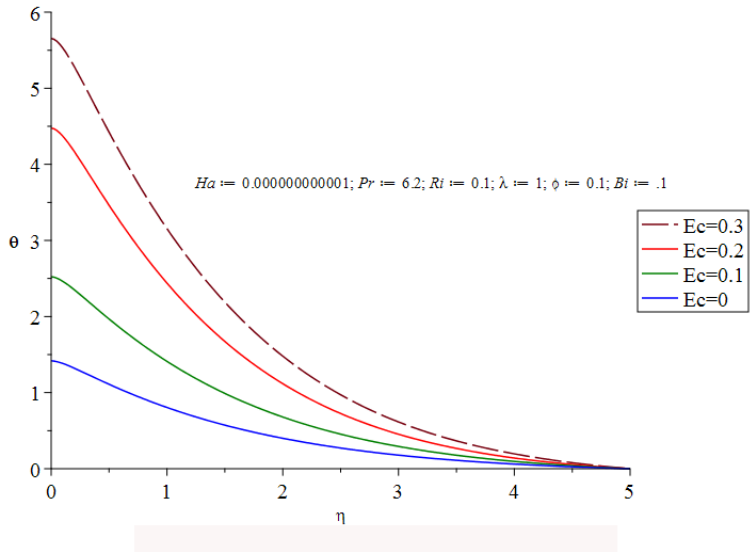

Figure 11: Temperature profiles for different Ec

From **table 3**, it is also observed that the rate of heat transfer - $\theta(\eta)$ at the surface of the plate $\eta = 0$ decreases as the as the nanoparticle volume fraction parameter ϕ increases. This observation is made for three different types of water based nanofluids. In addition, TiO_2-water nanofluid records the highest rate of heat transfer - $\theta(\eta)$ than in Cu-water and Al_2O_3-water.

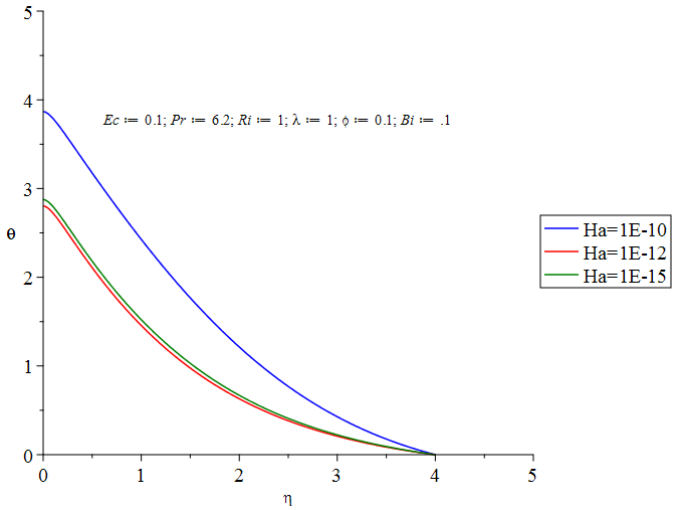

Figure 12: Temperature profiles for different Ha

Table 3: shear stress f"(0)and rate of heat transfer θ'(0)at the plate surface $\eta = 0$

ϕ	Cu-water		Al_2O_3-water		TiO_2-water	
	-f"(0)	$-\theta'(0)$	-f"(0)	$-\theta'(0)$	-f"(0)	$-\theta'(0)$
0.00	1.79719	0.09762	1.79719	0.09762	1.79719	0.09762
0.05	1.89955	0.09730	1.80634	0.09741	1.81160	0.09743
0.10	1.96291	0.09718	1.80194	0.09710	1.81141	0.09724
0.15	1.99449	0.09696	1.78591	0.09697	1.79826	0.09695
0.20	1.99964	0.09673	1.75975	0.09674	1.77394	0.09685

4. Conclusion

Based on the obtained graphical and tabular results, the following conclusions can be summarized as follows:

- The velocity of nanofluid increases as the strength of magnetic field decreases. The velocity of nanofluid flow can be enhanced by suitably controlling the intensity of the external magnetic field.
- The fluid velocity enhances in the presence of uniform magnetic field, whereas as the volume fraction parameter increases, the temperature of the fluid falls.
- The velocity and temperature of nanofluid decreases as a result of increasing unsteadiness parameter.
- The velocity and the temperature distributions decrease by decreasing Biot number.
- The shear stress and the rate of heat transfer at the surface enhances as a result of increasing nanoparticle volume fraction.
- The rate of heat transfer at the surface of the sheet is higher in case TiO2-water nanofluid than in Al2O3- water and Cu-water based nanofluids.

References

[1] S. U. Choi and J. A. Eastman, "Enhancing thermal conductivity of fluids with nanoparticles," Argonne National Lab., IL (United States), Tech. Rep., 1995.

[2] C. T. Nguyen, G. Roy, C. Gauthier, and N. Galanis, "Heat transfer enhancement using al 2 o 3–water nanofluid for an electronic liquid cooling system," *Applied Thermal Engineering*, vol. 27, no. 8, pp. 1501–1506, 2007.

[3] X. Wang, X. Xu, S. U. Choi *et al.*, "Thermal conductivity of nanoparticle-fluid mixture," *Journal of thermophysics and heat transfer*, vol. 13, no. 4, pp. 474–480, 1999.

[4] J. A. Eastman, S. Choi, S. Li, W. Yu, and L. Thompson, "Anomalously increased effective thermal conductivities of ethylene glycol-based nanofluids containing copper nanoparticles," *Applied physics letters*, vol. 78, no. 6, pp. 718–720, 2001.

[5] L. Li, Y. Zhang, H. Ma, and M. Yang, "An investigation of molecular layering at the liquid-solid interface in nanofluids by molecular dynamics simulation," *Physics Letters A*, vol. 372, no. 25, pp. 4541–4544, 2008.

[6] M. M. Ghosh, S. Roy, S. K. Pabi, and S. Ghosh, "A molecular dynamics-stochastic model for thermal conductivity of nanofluids and its experimental validation," *Journal of nanoscience and nanotechnology*, vol. 11, no. 3, pp. 2196–2207, 2011.

[7] S. Choi, Z. Zhang, W. Yu, F. Lockwood, and E. Grulke, "Anomalous thermal conductivity enhancement in nanotube suspensions," *Applied physics letters*, vol. 79, no. 14, pp. 2252–2254, 2001.

[8] C. Sun, W.-Q. Lu, B. Bai, and J. Liu, "Anomalous enhancement in thermal conductivity of nanofluid induced by solid walls in a nanochannel," *Applied Thermal Engineering*, vol. 31, no. 17, pp. 3799–3805, 2011.

[9] J. S. Nam, P.-H. Lee, and S. W. Lee, "Experimental characterization of micro-drilling process using nanofluid minimum quantity lubrication," *International Journal of Machine Tools and Manufacture*, vol. 51, no. 7, pp. 649–652, 2011.

[10] S. Kakaç and A. Pramuanjaroenkij, "Review of convective heat transfer enhancement with nanofluids," *International Journal of Heat and Mass Transfer*, vol. 52, no. 13, pp. 3187–3196, 2009.

[11] J. Buongiorno, "Convective transport in nanofluids," *Journal of Heat Transfer*, vol. 128, no. 3, pp. 240–250, 2006.

[12] O. Makinde and A. Aziz, "Mhd mixed convection from a vertical plate embedded in a porous medium with a convective boundary condition," *International Journal of Thermal Sciences*, vol. 49, no. 9, pp. 1813–1820, 2010.

[13] W. Mutuku-Njane and O. Makinde, "Mhd nanofluid flow over a permeable vertical plate with convective heating," *Journal of Computational and Theoretical Nanoscience*, vol. 11, no. 3, pp. 667–675, 2014.

[14] O. Makinde, "Similarity solution of hydromagnetic heat and mass transfer over a vertical plate with a convective surface boundary condition," *International Journal of Physical Sciences*, vol. 5, no. 6, pp. 700–710, 2010.

[15] O. Haddad, "Fully developed free convection in open-ended vertical channels partially filled with porous material," *Journal of Porous Media*, vol. 2, no. 2, 1999.

[16] A. Barletta, "Analysis of combined forced and free flow in a vertical channel with viscous dissipation and isothermal-isoflux boundary conditions," *Journal of heat transfer*, vol. 121, no. 2, pp. 349–356, 1999.

[17] A. Barletta, M. Celli, E. Magyari, and E. Zanchini, "Buoyant mhd flows in a vertical channel: the levitation regime," *Heat and mass transfer*, vol. 44, no. 8, pp. 1005–1013, 2008.

[18] N. C. Sacheti, P. Chandran, A. K. Singh, and B. S. Bhadauria, "Transient free convective flow of a nanofluid in a vertical channel," *Int. J. Energy Technol*, vol. 4, pp. 1–7, 2012.

[19] W. A. Azhar, D. Vieru, and C. Fetecau, "Free convection flow of some fractional nanofluids over a moving vertical plate with uniform heat flux and heat source," *Physics of Fluids*, vol. 29, no. 8, p. 082001, 2017.

[20] M. Narahari and L. Debnath, "Unsteady magnetohydrodynamic free convection flow past an accelerated vertical plate with constant heat flux and heat generation or absorption," *ZAMM-Journal of Applied Mathematics and Mechanics/Zeitschrift für Angewandte Mathematik und Mechanik*, vol. 93, no. 1, pp. 38–49, 2013.

[21] M. Turkyilmazoglu, "Unsteady convection flow of some nanofluids past a moving vertical flat plate with heat transfer," *Journal of Heat Transfer*, vol. 136, no. 3, p. 031704, 2014.

[22] P. Loganathan, P. N. Chand, and P. Ganesan, "Transient natural convective flow of a nanofluid past a vertical plate in the presence of heat generation," *Journal of Applied Mechanics and Technical Physics*, vol. 56, no. 3, pp. 433–442, 2015.

[23] S. Das and R. Jana, "Natural convective magneto-nanofluid flow and radiative heat transfer past a moving vertical plate," *Alexandria Engineering Journal*, vol. 54, no. 1, pp. 55–64, 2015.

[24] M. Hamad, I. Pop, and A. M. Ismail, "Magnetic field effects on free convection flow of a nanofluid past a vertical semi-infinite flat plate," *Nonlinear Analysis: Real World Applications*, vol. 12, no. 3, pp. 1338–1346, 2011.

[25] H. Schlichting and K. Gersten, *Boundary-layer theory*. Springer, 2016.

[26] J. Merkin, "The effect of buoyancy forces on the boundary-layer flow over a semi-infinite vertical flat plate in a uniform free stream," *Journal of Fluid Mechanics*, vol. 35, no. 3, pp. 439–450, 1969.

[27] R. Hunt and G. Wilks, "On the behaviour of the laminar boundary-layer equations of mixed convection near a point of zero skin friction," *Journal of Fluid Mechanics*, vol. 101, no. 2, pp. 377–391, 1980.

[28] M. R. Safaei, G. Ahmadi, M. S. Goodarzi, A. Kamyar, and S. Kazi, "Boundary layer flow and heat transfer of fmwcnt/water nanofluids over a flat plate," *Fluids*, vol. 1, no. 4, p. 31, 2016.

[29] H. Tamim, S. Dinarvand, R. Hosseini, S. Khalili, and A. Khalili, "Mixed convection boundary-layer flow of a nanofluid near stagnation-point on a vertical plate with

effects of buoyancy assisting and opposing flows," *Res J Appl Sci Eng Technol*, vol. 6, no. 10, pp. 1785–1793, 2013.

[30] T. Grosan and I. Pop, "Axisymmetric mixed convection boundary layer flow past a vertical cylinder in a nanofluid," *International Journal of Heat and Mass Transfer*, vol. 54, no. 15, pp. 3139–3145, 2011.

[31] A. S. Butt and A. Ali, "A computational study of entropy generation in magnetohydrodynamic flow and heat transfer over an unsteady stretching permeable sheet," *The European Physical Journal Plus*, vol. 129, no. 1, p. 13, 2014.

[32] S. Ahmad, A. M. Rohni, and I. Pop, "Blasius and sakiadis problems in nanofluids," *Acta Mechanica*, vol. 218, no. 3-4, pp. 195–204, 2011.

[33] R. K. Tiwari and M. K. Das, "Heat transfer augmentation in a two-sided lid-driven differentially heated square cavity utilizing nanofluids," *International Journal of Heat and Mass Transfer*, vol. 50, no. 9, pp. 2002–2018, 2007.

[34] K. Khanafer, K. Vafai, and M. Lightstone, "Buoyancy-driven heat transfer enhancement in a two-dimensional enclosure utilizing nanofluids," *International journal of heat and mass transfer*, vol. 46, no. 19, pp. 3639–3653, 2003.

[35] H. F. Oztop and E. Abu-Nada, "Numerical study of natural convection in partially heated rectangular enclosures filled with nanofluids," *International journal of heat and fluid flow*, vol. 29, no. 5, pp. 1326–1336, 2008.

[36] S. Kakaç and A. Pramuanjaroenkij, "Review of convective heat transfer enhancement with nanofluids," *International Journal of Heat and Mass Transfer*, vol. 52, no. 13, pp. 3187–3196, 2009.

[37] J. Buongiorno, "Convective transport in nanofluids," *Journal of Heat Transfer*, vol. 128, no. 3, pp. 240–250, 2006.

[38] A. S. Butt and A. Ali, "Entropy analysis of magnetohydrodynamic flow and heat transfer over a convectively heated radially stretching surface," *Journal of the Taiwan Institute of Chemical Engineers*, vol. 45, no. 4, pp. 1197–1203, 2014.

[39] T. Y. Na, *Computational methods in engineering boundary value problems*. Academic Press, 1980, vol. 145.

[40] A. Remeli, N. Arifin, F. Ismail, and I. Pop, "Marangoni-driven boundary layer flow in a nanofluid with suction and injection," *World Applied Sciences Journal*, vol. 17, pp. 21–26, 2012.

[41] D. B. Meade, B. S. Haran, and R. E. White, "The shooting technique for the solution of two-point boundary value problems," *Maple Technical Newsletter*, vol. 3, no. 1, pp. 1–8, 1996.

[42] M. H. Abolbashari, N. Freidoonimehr, F. Nazari, and M. M. Rashidi, "Entropy analysis for an unsteady mhd flow past a stretching permeable surface in nanofluid," *Powder Technology*, vol. 267, pp. 256–267, 2014.